International Journal of Control and Automation
Vol. 9, No. 9 (2016), pp.69-78
http//dx.doi.org/10.14257/ijca.2016.9.9.08

Research on the Low Voltage Ride-through Control Strategy based on State Feedback Linearization

Cuifeng Shen

School of Electrical Engineering, Yancheng Institute of Technology
Yancheng 224051, China
shencfycit@126.com

Abstract

Based on the analysis of on the dynamic mathematical model of double-fed wind turbines, exact non-linear state feedback linearization control method is adopted to design the control strategy of the LVRT (low voltage ride-through). Firstly, we select the output functions according to control target, and formulate the nonlinear system including input and output. Then, by using linearization the state feedback and using proper coordinate transforming, we convert this nonlinear system to the linear and controllable system. Finally, we finish the control strategy of the control system through the optimized linear control strategy. This control strategy only depend on the parameters of the wind turbines, and strengthen the robust of the parameters of control strategies.

Keywords*: Double-fed induction generator, voltage sag, state feedback linearization, low voltage ride through, electromagnetic torque, control of the reactive current*

1. Introduction

As can be seen from the literatures both at home and abroad, recently, most double fed system build the motor mathematical model in synchronous rotating frame. We can find the steady-state decoupling model of active and reactive power by simplifying it. Vector control is adopted, and conventional PI controller is used to control the double-fed induction generator, realizing the independent regulation of active and reactive power. Although, the control algorithm may make the current regulation become relative simple, double-fed induction generator is a nonlinear system. If conventional PI controller is adopted, it will cause poor dynamic characteristics, and it is difficult to reach the ideal control effect [1-3].

The nonlinear control strategy based on the exact state feedback linearization is adopted in this paper. The rotor side controller of double-fed induction generator wind turbine is designed, making the double-fed machine have better dynamic performances. It realizes the double-fed machine completely decoupling under both steady and dynamic situations. Meanwhile, this paper study the coordination control strategy of double PWM converters when the grid fault occurs, reducing the oscillation of motor, and improving the generator wind turbine dynamic performances.

2. Mathematical Model of DFIG (Double-Fed Induction Generator) Under D-Q Coordinates [4-6]

2.1. The Structure of Double-Fed Wind Generator System

The stator of double-fed wind generator system is directly connected to the grid, and the rotor realizes AC excitation by using the three-phase inverter, as is shown in Figure 1.

ISSN: 2005-4297 IJCA

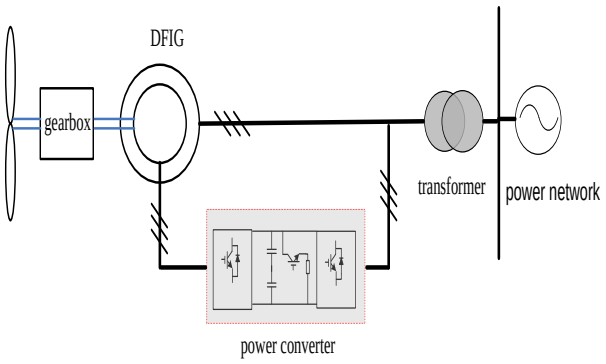

Figure 1. Double-fed Wind Generator System

2.2. Mathematical Model of Double-Fed Induction Generator

The voltage equation is

$$\begin{cases} u_{sd} = -R_s i_{sd} - p\psi_{sd} + \omega_1 \psi_{sq} \\ u_{sq} = -R_s i_{sq} - p\psi_{sq} - \omega_1 \psi_{sd} \\ u_{rd} = R_r i_{rd} + p\psi_{rd} - \omega_2 \psi_{rq} \\ u_{rq} = R_r i_{rq} + p\psi_{rq} + \omega_2 \psi_{rd} \end{cases} \quad (1)$$

The flux linkage equation is

$$\begin{cases} \psi_{sd} = L_s i_{sd} - L_m i_{rd} \\ \psi_{sq} = L_s i_{sq} - L_m i_{rq} \\ \psi_{rd} = L_r i_{rd} - L_m i_{sd} \\ \psi_{rq} = L_r i_{rq} - L_m i_{sq} \end{cases} \quad (2)$$

The electromagnetic torque equation is

$$T_e = n_p(\psi_{sq} i_{sd} - \psi_{sd} i_{sq}) = n_p L_m (i_{sd} i_{rq} - i_{sq} i_{rd}) \quad (3)$$

Where,

$u_{sd}, u_{sq}, u_{rd}, u_{rq}$: stator and rotor voltage at d-q axis,

$i_{sd}, i_{sq}, i_{rd}, i_{rq}$: stator and rotor current at d-q axis,

$\psi_{sd}, \psi_{sq}, \psi_{rd}, \psi_{rq}$: stator and rotor flux at d-q axis,

R_s, L_s: stator resistance and self-inductance,

R_r, L_r: rotor resistance and self-inductance,

L_m: mutual inductance,

ω_1: rotational angular velocity of d-q coordinate,

$\omega_2 = \omega_1 - \omega_r$: relative angular velocity of d-q coordinate to rotor,

The above equations constitute the mathematical model of double-fed induction generator at d-q axis. There is still coupling effect, especially the coaxial winding have a close relation to each other. But compared with the motor model at three-phase coordinates, nonlinear factors decreased significantly, which is the final purpose of coordinate transformation. It also lays the foundation for the following analysis of the vector control strategy of double-fed motor.

3. Design of the Rotor-Side Converter Nonlinear Controller

DFIG control model can be written in standard affine nonlinear, shown in Equation.4.

$$\begin{cases} \dot{\boldsymbol{x}} = \boldsymbol{f}(\boldsymbol{x}) + \boldsymbol{g}_1(\boldsymbol{x})u_1 + \boldsymbol{g}_2(\boldsymbol{x})u_2 = \boldsymbol{f}(\boldsymbol{x}) + \boldsymbol{g}(\boldsymbol{x})\boldsymbol{u} \\ y_1 = h_1(\boldsymbol{x}) \\ y_2 = h_2(\boldsymbol{x}) \end{cases} \tag{4}$$

Where, state variables are selected as

$$\boldsymbol{x} = \begin{bmatrix} x_1 \\ x_2 \end{bmatrix} = \begin{bmatrix} i_{rd} \\ i_{rq} \end{bmatrix} \tag{5}$$

In addition, the rotor voltage is directly controlled variable in double-fed induction generator. Therefore, the d-q component of rotor is set as the input variables, where

$$u = \begin{bmatrix} u_1 \\ u_2 \end{bmatrix} = \begin{bmatrix} u_{rd} \\ u_{rq} \end{bmatrix} \tag{6}$$

$$f(x) = \begin{bmatrix} f_1(x) \\ f_2(x) \end{bmatrix} = \begin{bmatrix} -\dfrac{R_r}{\sigma L_r} i_{rd} + \omega_s i_{rq} \\ -\dfrac{R_r}{\sigma L_r} i_{rq} - \omega_s i_{rd} + \omega_s \dfrac{L_m U_s}{\sigma L_r L_s \omega_1} \end{bmatrix} \tag{7}$$

$$\boldsymbol{g}(\boldsymbol{x}) = \begin{bmatrix} \boldsymbol{g}_1(\boldsymbol{x}) & \boldsymbol{g}_2(\boldsymbol{x}) \end{bmatrix} = \begin{bmatrix} \dfrac{1}{\sigma L_r} & 0 \\ 0 & \dfrac{1}{\sigma L_r} \end{bmatrix} \tag{8}$$

Because the active power and reactive power of DFIG stator side are the control targets of the motor, when the grid voltage is normal, they are selected as output variables.

$$\begin{cases} y_1 = h_1(\boldsymbol{x}) = P_s - P_{s0} = -\dfrac{3}{2}\dfrac{L_m}{L_s} U_s i_{rq} - P_{s0} \\ y_2 = h_2(\boldsymbol{x}) = Q_s - Q_{s0} = -\dfrac{3}{2}\dfrac{U_s^2}{L_s \omega_1} - \dfrac{3}{2}\dfrac{L_m}{L_s} U_s i_{rd} - Q_{s0} \end{cases} \tag{9}$$

Where,

y: the output variable when the grid voltage is normal,

Ps: stator active power,

P_{S0}: reference value of stator active power,

Q_s: stator reactive power,

Q_{s0}: reference value of stator reactive power.

When the grid voltage drops, the output variables of the system are selected as

$$\begin{cases} y_{f1} = h_{f1}(\boldsymbol{x}) = P_{fs} - P_{fs0} = -\dfrac{3}{2}\dfrac{L_m}{L_s}(U_s - \Delta U) i_{rq} - \dfrac{(U_s - \Delta U)}{U_s} P_{s0} \\ y_{f2} = h_{f2}(\boldsymbol{x}) = Q_{fs} - Q_{fs0} = -\dfrac{3}{2}\dfrac{(U_s - \Delta U)^2}{L_s \omega_1} - \dfrac{3}{2}\dfrac{L_m}{L_s}(U_s - \Delta U) i_{rd} - \dfrac{(U_s - \Delta U)}{U_s}(S_0 - P_{s0}) \end{cases} \tag{10}$$

Where,

y_f : output variable when the grid voltage fault occurs,

P_{fs}: stator active power when the grid voltage fault occurs,

P_{fs0}: reference value of stator active power when the grid voltage fault occurs,

Q_{fs}: stator reactive power when the grid voltage fault occurs,

Q_{fs0}: reference value of stator reactive power when the grid voltage fault occurs.

ΔU_s: motor stator voltage drop quantity

S_0: motor rated capacity

Through coordinate transformation, affine nonlinear system (Equation.4) is transformed into the linear system described by Z. When the grid is at normal and fault state, it can be obtained as follows

$$\dot{\boldsymbol{z}} = \boldsymbol{A}\boldsymbol{z} + \boldsymbol{B}\boldsymbol{v} \tag{11}$$

$$\dot{\boldsymbol{z}}_{\boldsymbol{f}} = \boldsymbol{A}_{\boldsymbol{f}}\boldsymbol{z}_{\boldsymbol{f}} + \boldsymbol{B}_{\boldsymbol{f}}\boldsymbol{v}_{\boldsymbol{f}} \tag{12}$$

Where,

$$\boldsymbol{A} = \boldsymbol{A}_{\boldsymbol{f}} = [\boldsymbol{0}], \boldsymbol{A} = \boldsymbol{B}_{\boldsymbol{f}} = \begin{bmatrix} 1 & 0 \\ 0 & 1 \end{bmatrix}, \boldsymbol{v} = \begin{bmatrix} v_1 \\ v_2 \end{bmatrix}, \boldsymbol{v}_{\boldsymbol{f}} = \begin{bmatrix} v_{f1} \\ v_{f2} \end{bmatrix}$$

According to Equation.9 and Equation.10, the relationship between $\boldsymbol{u}$ and $\boldsymbol{v}$ can be drawed as follows

$$\begin{bmatrix} v_1 \\ v_2 \end{bmatrix} = \boldsymbol{A}(\boldsymbol{z}) + \boldsymbol{B}(\boldsymbol{z}) \begin{bmatrix} u_1 \\ u_2 \end{bmatrix} \tag{13}$$

Where,

$$\boldsymbol{A}(\boldsymbol{z}) = \begin{bmatrix} \boldsymbol{L}_{\boldsymbol{f}} h_1(\boldsymbol{x}) \\ \boldsymbol{L}_{\boldsymbol{f}} h_2(\boldsymbol{x}) \end{bmatrix} = \begin{bmatrix} -\frac{3}{2}\frac{L_m}{L_s} U_s \left(-\frac{R_r}{\sigma L_r} i_{rq} - \omega_s i_{rd} + \omega_s \frac{L_m U_s}{\sigma L_r L_s \omega_1} \right) \\ -\frac{3}{2}\frac{L_m}{L_s} U_s \left(-\frac{R_r}{\sigma L_r} i_{rd} + \omega_s i_{rq} \right) \end{bmatrix} \tag{14}$$

$$\boldsymbol{B}(\boldsymbol{z}) = \begin{bmatrix} 0 & -\frac{3}{2}\frac{U_s L_m}{\sigma L_r L_s} \\ -\frac{3}{2}\frac{U_s L_m}{\sigma L_s L_r} & 0 \end{bmatrix} \tag{15}$$

According to Equation.13, the control variables can be drawed as follows

$$\begin{bmatrix} u_1 \\ u_2 \end{bmatrix} = \boldsymbol{D}(\boldsymbol{x}) \left[-\boldsymbol{A}(\boldsymbol{z}) + \begin{bmatrix} v_1 \\ v_2 \end{bmatrix} \right] \tag{16}$$

$$\boldsymbol{D}_{\boldsymbol{f}}(\boldsymbol{x}) = \boldsymbol{B}_{\boldsymbol{f}}(\boldsymbol{z})^{-1} = \begin{bmatrix} 0 & -\frac{2}{3}\frac{\sigma L_s L_r}{(U_s - \Delta U) L_m} \\ -\frac{2}{3}\frac{\sigma L_s L_r}{(U_s - \Delta U) L_m} & 0 \end{bmatrix} \tag{17}$$

Set

$$\boldsymbol{v}^* = \begin{bmatrix} -1 & 0 \\ 0 & -1 \end{bmatrix} \begin{bmatrix} z_1 \\ z_2 \end{bmatrix} \tag{18}$$

$$\boldsymbol{v}_f^* = \begin{bmatrix} -1 & 0 \\ 0 & -1 \end{bmatrix} \begin{bmatrix} z_{f1} \\ z_{f2} \end{bmatrix} \tag{19}$$

Substitute Equation.14 to Equation.12, then the control strategy can be drawed as follows

$$\begin{cases} u_{rd} = \dfrac{2}{3}\dfrac{\sigma L_s L_r}{U_s L_m}\left[-\dfrac{3U_s L_m}{2L_s}\left(-\dfrac{R_r}{\sigma L_r} i_{rd} + \omega_s i_{rq}\right) + Q_s - Q_{s0}\right] \\ u_{rq} = \dfrac{2}{3}\dfrac{\sigma L_s L_r}{U_s L_m}\left[-\dfrac{3U_s L_m}{2L_s}\left(-\dfrac{R_r}{\sigma L_r} i_{rq} - \omega_s i_{rd} + \omega_s \dfrac{L_m U_s}{\sigma L_r L_s \omega_1}\right) + P_s - P_{s0}\right] \end{cases} \tag{20}$$

Substitute Equation.19 to Equation.21, then the control strategy can be drawed as follows

$$\begin{cases} u_{frd} = \dfrac{2}{3}\dfrac{\sigma L_s L_r}{(U_s - \Delta U) L_m}\left[-\dfrac{3(U_s - \Delta U) U_s L_m}{2L_s}\left(-\dfrac{R_r}{\sigma L_r} i_{rd} + \omega_s i_{rq}\right)\right. \\ \qquad \left. + Q_{fs} - \dfrac{(U_s - \Delta U)}{U_s}(S_0 - P_{s0})\right] \\ u_{frq} = \dfrac{2}{3}\dfrac{\sigma L_s L_r}{(U_s - \Delta U) L_m}\left[-\dfrac{3(U_s - \Delta U) L_m}{2L_s}\left(-\dfrac{R_r}{\sigma L_r} i_{rq} - \omega_s i_{rd} + \omega_s \dfrac{L_m (U_s - \Delta U)}{\sigma L_r L_s \omega_1}\right)\right. \\ \qquad \left. + P_{fs} - \dfrac{(U_s - \Delta U)}{U_s} P_{s0}\right] \end{cases} \tag{21}$$

According to Equation.20 and Equation.21, the state feedback linear control method has the relationship to DFIG own parameters. This method is used to regulate the voltage of RSC, so as to control the slip of motor and the stator active and reactive power. The block of double fed control scheme is shown in Figure 2.

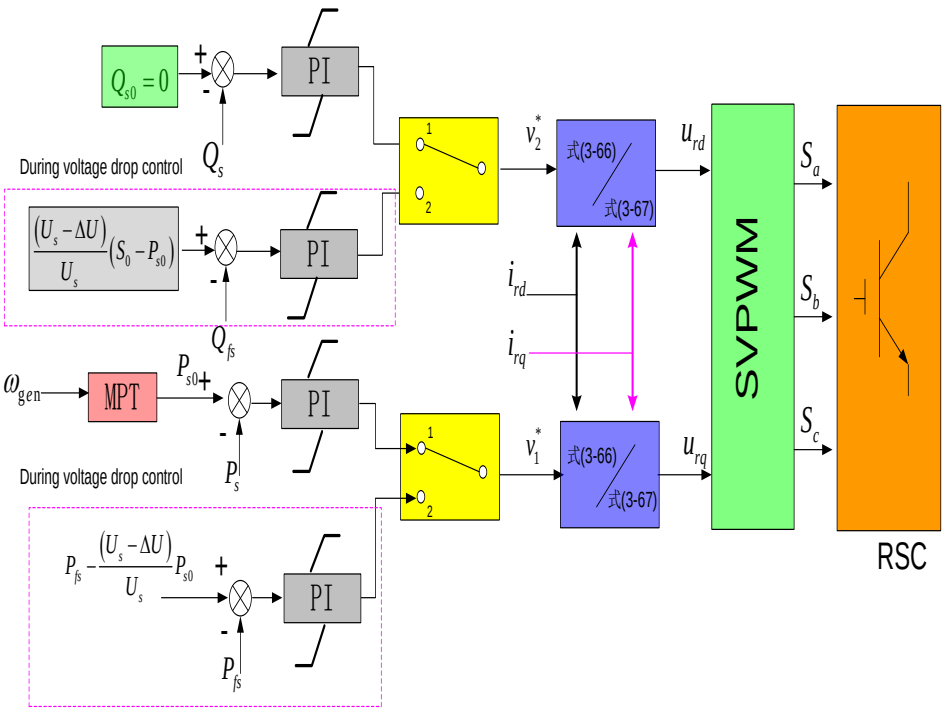

Figure 2. The Block of Coordinated Control based on Exact Feedback Linearization

4. Simulation Results and Analysis [7-10]

Under normal and fault conditions of the grid, the double-fed wind generator system model is built in PSCAD/EMTDC, so as to evaluate the control strategy based on the exact state feedback linearization and the performance of controller designed. Simulation parameters are given as follows: three-phase voltage effective amplitude 690v, frequency 50Hz, three-phase line inductance 5mH, three-phase line resistance 0.15Ω, DC bus capacitance 18000uF, DC bus rated voltage 1200V, number of pole pairs n_p=1, synchronous speed 3000rpm, rated power P_n=2MW, rated voltage U_n=690V, rated frequency fn=50Hz, stator resistance Rs=0.00488p.u., rotor resistance Rr=0.00549p.u., stator leakage reactance Lσs=0.1386p.u., rotor leakage reactance Lσr=0.1493p.u., moment of inertia H=3.5s., the transformation ratio between stator and rotor Ns/Nr=0.45.

Simulation experiments are done to validate the performance of the nonlinear control strategy based on the exact state feedback linearization, traditional PI control of simulation results are also given as comparison. When the grid fault occurs, the dynamic response of active power and reactive power coordination control are compared. The dynamic response of the maximum wind power tracking control are also compared.

Before the grid fault occurs, the wind speed is 8 m/s at the horizontal axis. When the motor is running at sub-synchronous speed, the output active and reactive power of DFIG are respectively 1.2MW and 0. The voltage falls at t=2s, and the drop depth is 50%, lasting time is 5s. The stator voltage simulation result is shown in Figure.3.

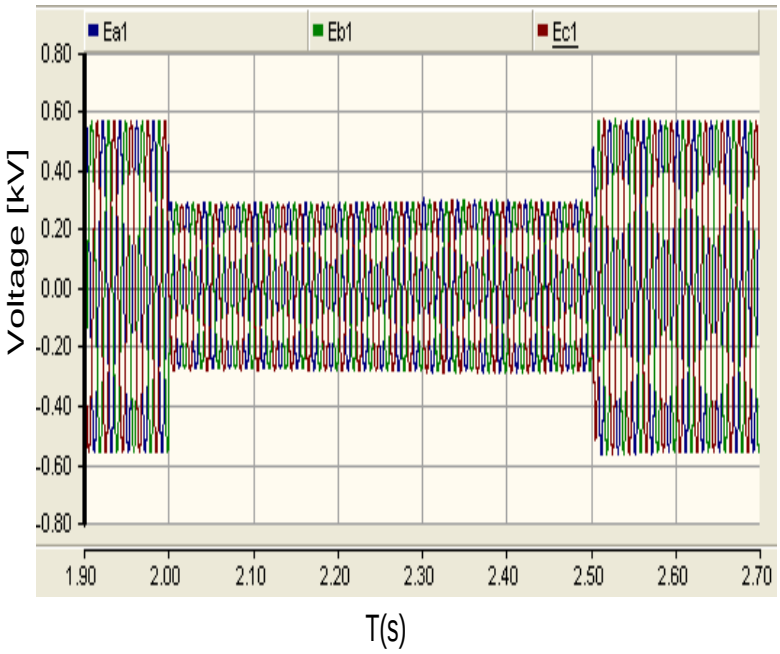

Figure 3. The Stator Voltage of DFIG

Figure.4 are the power comparison results under nonlinear coordinated control and traditional PI control. Figure4 (a) is active power, and Figure4 (b) is reactive power. Because the grid voltage falls 50%, the active power of stator output drops from 1.2MW to 0.6MW with the two different control strategies. As can be seen from the simulation results, when the grid occurs fault, traditional PI control strategy can not get controlled target value, due to the output saturation of PI controller. Because there may be surge current in the system, the output of PI controller must be saturated. When the grid fault is cleared at t=2.5s, the voltage returns to normal. There is obvious overshoot phenomenon of the active power, when traditional PI controller is adopted, and the highest value is 1.5

times the normal value. But when the nonlinear coordinated control strategy is adopted, there is no overshoot phenomenon. Figure4(b) shows the reactive power comparison results with the two control strategies. The reactive power get the maximum value 0.5Mvar at 0.05s, and become stable 0.4Mvar at 0.2s. But when traditional PI control is adopted, the reactive power exists over damping state, and become stable 0.4Mvar at 0.3s. Therefore, as for reactive power, nonlinear coordinated control strategy have faster dynamic response by contrast the two control strategies. It can meet the control requirements of reactive power, when the power system occur faults. It has the same control effect as active power. When the grid fault is cleared and grid voltage is recovered, the traditional PI controller will lead to a significant overshoot response of reactive power. In general, by the contrast of power results, the control performances with nonlinear coordinated control strategy are better than traditional PI, as is shown in Figure.4.

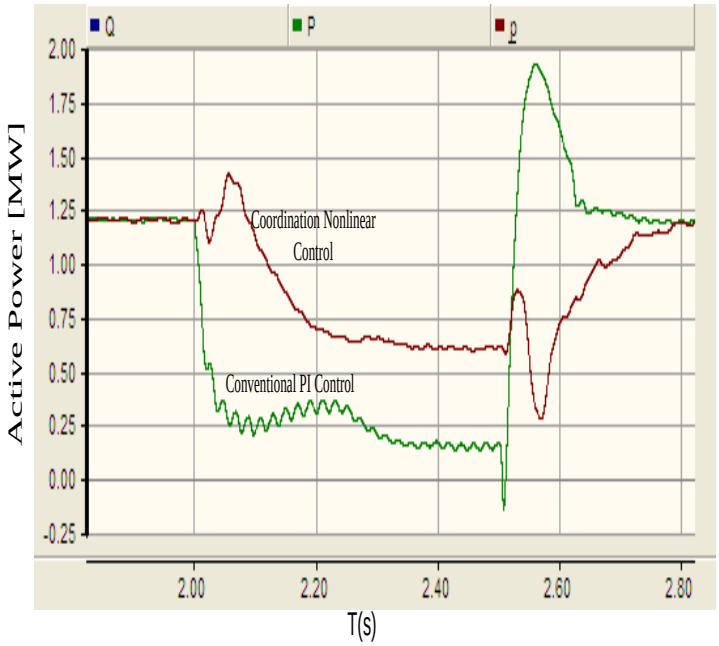

(a) active power

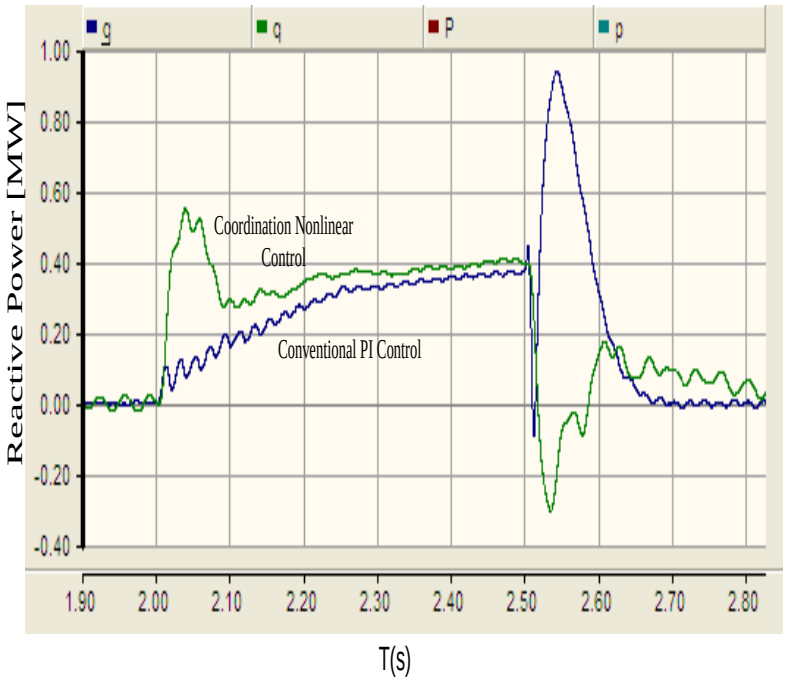

(b)Reactive power

Figure 4. The Comparison of Power between Nonlinear Coordinate Control and Traditional PI Control

4. Conclusion

There is coupling effect between three-phase voltage-fed PWM converter and DFIG, which is nonlinear, strong coupling, multi variable and complex system. Common decoupling control methods have disadvantages. The exact state feedback linearization theory are more and more widely used in control system, especially in the scope of power electronics, realizing the high performance decoupling control between converter and motor. This paper designed the power coordinated control low voltage ride through control strategy based on state feedback exact linearization. The output function is selected by control objective, and then use state feedback linearization and suitable coordinate transformation to change the nonlinear system into linear controllable system. Finally, the control strategy of the system is designed by linear optimal control method.

When the grid voltage is normal, the method designed is compared with vector control based on traditional PI regulator and state feedback linearization control strategy. As can be seen from the simulation results, when the grid voltage occur faults, the active and reactive power of DFIG under nonlinear power coordination control strategy, the dynamic response is obviously better than that of vector control based on PI regulator. The future work is to design a 7.5KW variable speed constant frequency doubly-fed wind power system laboratory platform. On this laboratory platform, the experiment results are expected to show agreement with the theoretical analysis.

References

[1] C. W. Lin, F. X. Wang and X. J. Yao, "Study on excitation control of VSCF doubly fed wind power generator", Proceedings of the CSEE, vol. 23, no. 11, **(2003)**, pp. 122-125.
[2] A.Petersson, S.Lundberg and T.Thiringer, "Comparison between stator-flux and grid-flux-oriented rotor current control of doubly-fed induction generators, 35th Annual IEEE Power Electronics Specialists Conference, **(2004)**, pp. 482-486.
[3] W. Wang, M. D. Sun and X. D. Zhu, "Analysis on the low voltage ride through technology of DFIG", Automation of Electric Power Systems, vol. 31, no. 23, **(2007)**, pp. 84-89.
[4] J. B. Hu and Y. K. He, "Low voltage ride through operation and control of doubly fed induction generator wind turbines", Automation of Electric Power Systems, vol. 32, no. 2, **(2008)**, pp. 49-52.
[5] J.Niiranen, "Voltage ride through of a doubly-fed generator equipped with an active crowbar", 11th International Power Electronics and Motion, Control Conference, **(2004)**, pp. 56-59.
[6] W. Zhang, P. Zhou and Y. He, "Analysis of the by-pass resistance of an active crowbar for doubly-fed induction generator based wind turbines under grid faults", International Conference on Electrical Machines and Systems ICEMS, **(2008)**, pp. 2316-2321.
[7] J. Yao, Y. Liao and J. P. Tang, "Ride-through control strategy of AC excited wind-power generator for grid short-circuit fault", Proceedings of the CSEE, vol. 27, no. 30, **(2007)**, pp. 64-71.
[8] D. W. Xiang, S. C. Yang and L. Ran, "Ride-through control strategy of a doubly fed induction generator for symmetrical grid fault", Proceedings of the CSEE, vol. 26, no. 3, **(2006)**, pp. 164-170.
[9] J. Yao, "Study on control strategies of AC excited generator and its excitation power supply, Ph.D. Dissertation of Chongqing University, **(2007)**.
[10] C. Zhan and C. D. Barker, "Fault ride-through capability investigation of a doubly-fed induction generator with an additional series-connected voltage source converter", The 8th IEE International Conference on AC and DC Power Transmission, **(2006)**, pp. 380-386.